

0945060134 – 1

Source Identification, Counterparts and Properties

STONKS alert

This source is the same as: **0945060133 – 5**.

- Type of Alert: First Detection,
- Long-term Variability = 11.9 for **0945060134 – 1** and 11.4 for **0945060133 – 5**,
- No short-term Variability.

The long-term variability is the difference between the upper limit of the flux lowest value and the lower limit of the flux highest value.

The short-term variability is the result of a χ^2 test of the flux against a constant value.

In the remainder of this document and for reasons of clarity and simplicity, we will refer to source **0945060134 – 1** as **34-1** and to source **0945060133 – 5** as **33-5**.

XMM-Newton Science Archive

<https://nxs.a.esac.esa.int/nxs-a-web/#search>

Simbad

The source is not identified on Simbad.

ESASky

<https://sky.esa.int/esasky/?target=53.59466666666666%20-28.902777777777782&hips=DSS2+color&fov=1&projection=SIN&cooframe=J2000&sci=true&lang=fr>

There is no EPIC Stack pointer on this source because it is not updated yet as the source is too new.

The source has multiple counterparts on ESASky:

- XMM-SUSS 6.2 (UV to Optical)? Slightly off,
- Gaia DR3 (Optical),
- Euclid MER Q1 (Optical to Near-IR),
- 2MASS (Near-IR),
- ALLWISE (Near-IR to Mid-IR).

Gaia DR3 gives the following useful data:

- Parallax: $P = 2.941 \text{ mas} \rightarrow d \approx 340 \text{ pc}$,
- Magnitude: $G = 19.6951$,
- $G_{BP} - G_{RP} = 2.416$.

The source is faint and most likely Galactic.

Gaia DR3 also gives a probability of classification:

- Classprob Dsc Combmod Galaxy = $9.9688 * 10^{-13}$,
- Classprob Dsc Combmod Quasar = $9.0908 * 10^{-13}$,
- Classprob Dsc Combmod Star = 1.

The source is classified as a **star**.

There is no publication.

3DNH-tool

<http://astro.uni-tuebingen.de/nh3d/nhtool>

3DNH-tool suggests a column density of $n_H \approx 3 * 10^{20} \text{ cm}^{-2}$, which is relatively low, typical of a Galactic source. However, this value might not be reliable as it does not account for the distance of the source.

X-ray Periodicity

Source 34-1

PN: Search with $f_0 \approx 0.0002 \text{ s}^{-1} \rightarrow P \approx 5000 \text{ s}$ and with $f_0 \approx 0.0001 \text{ s}^{-1} \rightarrow 5800 \text{ s}$.

MOS2: Search with $f_0 \approx 4.8 \text{ s}^{-1} \rightarrow P \approx 0.2 \text{ s}$, with $f_0 \approx 3.1 \text{ s}^{-1} \rightarrow P \approx 0.3 \text{ s}$ and with $f_0 \approx 1.2 \text{ s}^{-1} \rightarrow P \approx 0.8 \text{ s}$.

As the results differ between instruments, we chose to consider only those from the instrument with the highest maximum likelihood. According to the STONKS alert document, the maximum likelihood for PN is $DetML = 514.4$, while for M2 it is $DetML = 132.2$, supporting our decision to rely solely on the PN data.

Source 33-5

The source exhibits no periodicity originally but because it is the same source as 34-1, we did a search with the frequency f_0 found for this last.

PN: Search with $f_0 \approx 0.0001 \text{ s}^{-1} \rightarrow P \approx 10000 \text{ s}$. Same for **MOS1** and **MOS2**.

The search with $f_0 \approx 0.0002 \text{ s}^{-1}$ gave no results.

Discussion

The periodicity of 5000 s ($\sim 1.39 \text{ h}$) is consistent with a cataclysmic variable. Their orbital periods usually range from 4800 s to 36000 s ($\sim 80 \text{ min}$ to $\sim 10 \text{ h}$); There is even a known “period gap” between 7200 s and 10800 s ($\sim 2\text{--}3 \text{ h}$) but systems still exist within and around this range.

A 5000 s periodicity falls well within the CV orbital period regime, particularly on the shorter end, which is common for:

- Non-magnetic CVs (e.g., dwarf novae in quiescence)
- AM CVn systems (ultracompact helium-transferring binaries)

In magnetic CVs (e.g., intermediate polars), the white dwarf’s spin period can often be detected as a strong X-ray periodicity.

- Typical spin periods range from a few hundred to several thousand seconds.
- A 5000 s modulation could also represent the spin period in such a system.

X-ray Spectral Properties

Xspec models

The main models that we are using are: Black body, Bremsstrahlung, Apec, Powerlaw and Gauss, or a combination of two components: Black body and Powerlaw, Bremsstrahlung and Powerlaw, Gauss and Powerlaw, and, Apec and Apec.

Black body

When an X-ray spectrum is well fitted by a black body model, it suggests that the X-ray emission is coming from a hot, dense surface or region that radiates like an ideal thermal emitter (i.e. a black body). A black body emits radiation with a spectrum that depends only on its temperature, and this emission is:

- Smooth and has a characteristic peak at a certain energy,
- Thermal, meaning it reflects a state of thermal equilibrium,
- Strongly dependent on temperature (the hotter the black body, the more it emits and the higher the peak energy).

A black body model fit generally implies that the X-rays are emitted by a compact and hot surface (not by diffuse gas). Likely sources include:

- The surface of a neutron star,
- The boundary layer in a white dwarf system (e.g., in cataclysmic variables),
- The accretion disk's inner region (if dense and hot enough),
- Or even a hot stellar photosphere.

Bremsstrahlung

When a bremsstrahlung model (also known as thermal bremsstrahlung or free-free emission) fits an X-ray spectrum well, it suggests that the X-ray emission is primarily produced by hot, ionized gas (i.e. plasma) through a specific process: Bremsstrahlung (German for “braking radiation”) occurs when electrons are decelerated as they pass near atomic nuclei. This deceleration causes them to lose energy in the form of X-ray photons. This type of emission is thermal, meaning the spectrum depends on the temperature of the plasma. A good fit with this model indicates that:

- The X-ray source likely contains hot plasma.
- The X-ray spectrum is smooth and continuous, without strong emission lines (although lines may still be present if other processes are involved).

It is common in environments like:

- Accretion shocks (e.g., in cataclysmic variables, where infalling material heats up).
- Stellar coronae (like in active M-dwarfs).
- Supernova remnants or galaxy clusters.

Source of the plasma temperature: <https://www.sciencedirect.com/topics/earth-and-planetary-sciences/plasma-temperature>.

Astrophysical Plasma Emission Code (APEC)

When an X-ray spectrum is well fitted by an Apec model, it indicates that the emission is coming from a hot, diffuse, optically thin plasma in collisional ionization equilibrium. It models emission from a plasma that contains a mix of elements (H, He, Fe, etc.) at a certain temperature, where:

- Electrons collide with ions, exciting them,
- The ions then de-excite by emitting photons, often in the X-ray range,
- Both continuum emission (mainly bremsstrahlung) and emission lines are included in the model.

Thus, when Apec fits the spectrum, it suggests that:

- We are observing a thermal plasma (like bremsstrahlung, but with line emissions),
- The plasma is optically thin (photons escape without being absorbed),
- The plasma is in collisional ionization equilibrium, meaning the ionization state is stable and set by the temperature.

It is common in environments like:

- Stellar coronae (like in active M-dwarfs),
- Supernova remnants,
- Hot gas in galaxy clusters,
- Accretion disks or shocks in systems like cataclysmic variables (CVs),
- Flares, where gas is suddenly heated and emits thermal X-rays.

Powerlaw

When an X-ray spectrum is well fit by a powerlaw model, it means that the emission is of non-thermal origin, meaning that it doesn't come from a hot gas or a thermal surface like in blackbody or bremsstrahlung models. Instead, it points to processes involving high-energy particles, such as acceleration or scattering. Mathematically, a powerlaw has the form:

$$F(E) \propto E^{-\Gamma} \quad (1)$$

With $F(E)$ the flux of photon at energy E and Γ the photon index (PhoIndex in *Xspec*) typically between 1 and 3. A steeper index (higher Γ) means the spectrum drops off faster with energy.

A good powerlaw fit implies non-thermal emission mechanisms, such as:

- Synchrotron radiation (relativistic electrons spiralling in magnetic fields),
- Inverse Compton scattering (high-energy electrons boosting low-energy photons),
- Emission from accretion flows, like in black holes or neutron stars,
- Emission from magnetically active stars (e.g. in the tail of a flare event).

We might see a powerlaw spectrum from:

- Active Galactic Nuclei (AGN) because of the non-thermal emission from jets or corona,
- X-ray binaries because of the accretion-powered emission with comptonization,
- Pulsars or magnetars because of the synchrotron and curvature radiation,
- Some flare stars or M-dwarfs because of high-energy particles in flare tails,
- Cataclysmic variables (CVs) if there is a strong magnetic activity or shock jets.

Gauss

When an X-ray spectrum is well fit by a Gauss model, it means that one or more features in the spectrum, usually emission or absorption lines, are well described by a Gaussian function which is defined as:

$$f(E) = Ae^{-\frac{(E-E_0)^2}{2\sigma^2}} \quad (2)$$

Where E is the energy (in keV or eV), E_0 is the centroid energy (where the peak is), σ is the standard deviation, related to the line width and A is the amplitude, related to the line intensity.

A Gaussian profiles model spectral lines caused by atomic transitions if they are symmetric and not strongly broadened by complex physics (e.g., relativistic effects). So, if the spectrum is well fit by a Gauss model:

- There is likely a distinct emission or absorption line in the data,
- The line is symmetric and has a shape consistent with a Gaussian, suggesting relatively simple broadening mechanisms (e.g., thermal or instrumental),
- The Gaussian parameters can give physical information, such as:
 - Line center, which identifies the emitting/absorbing element or transition,
 - Line width, which gives insight into velocity dispersion, turbulence, or temperature,
 - Amplitude, which relates to the number of photons, hence the strength of the line.

Line centroid (E_0) can tell the ionization state of the emitting element. For example:

- $\sim 6.4 keV \rightarrow$ neutral Fe (fluorescent line from reflection),
- $\sim 6.7 keV \rightarrow$ He-like Fe ($Fe\ 55$),
- $\sim 6.97 keV \rightarrow$ H-like Fe ($Fe\ 56$).

Line width (σ) can reveal turbulence, bulk motion, or instrumental broadening. A very broad line might hint at high-velocity material or blending of multiple unresolved lines.

Line amplitude combined with the continuum, gives info on abundances, emission measure, or plasma conditions.

In CVs for example, a $Fe\ K\alpha$ line at around $\sim 6.4 keV$ might be modeled with a Gaussian as well as lines from other elements like O, Ne, Mg, Si. These lines are typically superimposed on the thermal continuum.

Seeing a Gaussian line in a CV spectrum might help confirm its identity. The Fe line complex is often used to distinguish magnetic CVs, especially intermediate polars, from other types of X-ray sources. Sometimes, a spectrum is fit with a thermal + one or more Gaussians to cleanly characterize both the continuum and the lines.

X-ray parameters

Here's a comparison table of the typical X-ray spectral parameters k_T (plasma temperature) and PhoIndex Γ (photon index of a power-law model) for cataclysmic variables (CVs), active stars, and active galactic nuclei (AGNs):

Source type	k_T (keV)	PhoIndex Γ	Notes
CV	- Cold component: $\sim 0.1 - 0.7 keV$ - Medium component: $\sim 4 - 10 keV$ - Hot component: $\sim 16 - 60 keV$	Not typically used; spectra are dominated by thermal emission	Multi-temperature plasma models are common, especially for magnetic CVs. Spectra often include multiple thermal components and a $6.4 keV Fe\ K\alpha$ line.

Active star	$\sim 0.1 - 3 \text{ keV}$	Not typically used; thermal models preferred	Emission arises from coronal plasma, often modeled with one or more thermal components. Power-law models are generally not applicable.
AGN	Not typically used; emission is non-thermal	$\sim 1.5 - 2.0$	X-ray spectra are dominated by non-thermal processes, modeled with a power-law. The photon index Γ typically ranges from 1.5 to 2.0.

Fit statistic

Chi-squared

The chi-squared fit statistic assumes that each bin contains enough events to approximate the Poisson distribution with a normal distribution. If some bins have under 20 counts, this test becomes unreliable. In order to be more secure, we will consider that if the bins have less than 100 counts, C-statistic should be used instead. Here, we have about 95 counts which under 100 but still close, so we will do both Chi-squared and C-statistic.

The Chi-squared χ^2 is the sum of the squared residuals, weighted by the errors in the data. The reduce Chi-squared χ^2_v (reduced by the number of degrees of freedom) is:

$$\chi^2_v = \frac{\chi^2}{n_{bins} - n_{parameter}} \quad (2)$$

- $\chi^2_v \approx 1$: Good fit.
- $\chi^2_v \gg 1$: Bad fit.
- $\chi^2_v \ll 1$: Overfitting?

Here, the number of bins is: $n_{bins} = 18$. The number of parameters $n_{parameter}$ depends on the model:

Model	$n_{parameter}$	Main parameters
tbabs*bbody	3	nH, kT, norm
tbabs*bremss	3	nH, kT, norm
tbabs*apec	4	nH, kT, abundance, norm
tbabs*powerlaw	3	nH, PhoIndex, norm
tbabs*(bbody+powerlaw)	5	nH, kT, norm (bbody), PhoIndex, norm (powerlaw)
tbabs*(bremss+powerlaw)	5	nH, kT, norm (bremss), PhoIndex, norm (powerlaw)
tbabs*(gauss+powerlaw)	6	nH, LineE, Sigma, norm (gauss), PhoIndex, norm (pow)
tbabs*(apec+apec)	6	nH, temp1, abundance, norm1, temp2, norm2

Let's compare the most promising models (i.e. with the chi-squared closest to 1):

Criteria	Bremsstrahlung	Power-law	Bremsstrahlung + Power-law	Gauss + Bremsstrahlung	Gauss + Power-law
Chi-squared χ^2	14.5160	15.0731	12.4011	11.5493	12.6865
Reduce Chi-squared χ^2_v (5 bins)	0.968	1.005	0.954	0.962	1.057

Column density $n_H (10^{22} \text{ cm}^{-2})$	4.669e-02 ± 2.631e-02	0.142 ± 5.123e-02	5.813e-02 ± 3.204e-02	4.864e-02 ± 2.673e-02	0.150 ± 5.333e-02
$k_T (keV)$	1.617 ± 0.42	X	1.380 ± 0.435	1.574 ± 0.409	X
PhoIndex Γ	X	2.600 ± 0.316	-2.500 ± 3.616	X	2.659 ± 0.329
Energy centroid <i>LineE</i> (keV)	X	X	X	6.5 (frozen)	6.7 (frozen)
Line width σ	X	X	X	1.559e-03 ±1.00	4.756e-09 ±- 1.00
Norm	2.007e-05 ± 4.406e-06	1.69e-05 ± 3.38e-06	2.259e-05 ± 6.481e-06 (bremss), 2.959e-09 ± 2.048e-08 (pow)	1.394e-06 ± 8.091e-07 (gauss), 2.047e-06 ± 4.602e-06 (bremss)	1.374e-06 ± 8.892e-07 (gauss), 1.742e-05 ± 3.579e-06 (pow)
Null hypothesis probability	4.868e-01	4.462e-01	4.951e-01	5.649e-01	4.723e-01
Degrees of freedom	15	15	13	13	13

The Power-law model has a $\chi^2_\nu = 1.005$ which is extremely close to 1, meaning it is almost a perfect fit. The other models are also very good fit.

The column density value given by the Bremsstrahlung, Bremsstrahlung + Power-law and Gauss + Bremsstrahlung models are the closest one to what 3DNH-tool suggest with $n_H \approx 5 * 10^{20} \text{ cm}^{-2}$. The values of the column density of the Power-law and Gauss + Power-law models are around: $n_H \approx 10^{21} \text{ cm}^{-2}$, indicating a slightly farer source but still coherent. All imply a Galactic source.

The models have temperatures $k_T \approx 1.4 - 1.6 \text{ keV}$, which is consistent with hot plasmas, indicating possible coronal activity or accretion.

The Power-law and Gauss + Power-law models model yield a photon index $\Gamma \approx 2.6$, which is rather soft, and therefore more typical of certain non-thermal sources or a spectrum dominated by the diffuse background (synchrotron, inverse Compton), whereas the Bremsstrahlung + Power-law model gives a photon index of $\Gamma \approx -2.5$ with quite high uncertainties, which is not a satisfying result.

The Bremss + Power-law and Gauss + Power-law models fit best for the energy centroid set to *LineE* = 6.5 keV and *LineE* = 6.7 keV which correspond to *Fe* 55. However, on the spectrum these values are between a point at 5 keV and a point at 8 keV, so a 3 keV gap is too large to conclude about the presence of an iron line (which is very narrow).

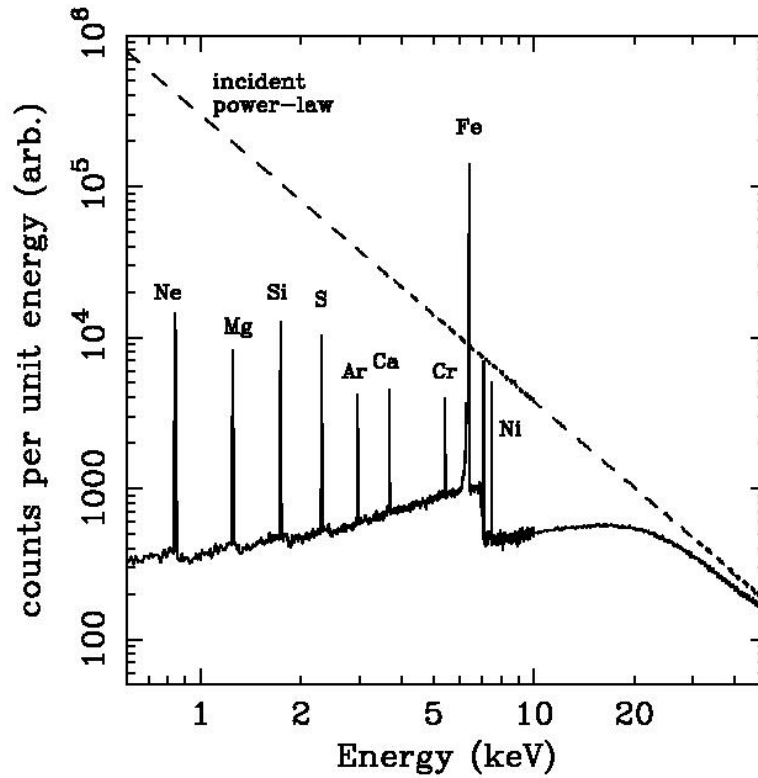


Figure 1. X-ray reflection from an illuminated slab. Dashed line shows the incident continuum and solid line shows the reflected spectrum (integrated over all angles). Monte Carlo simulation from Reynolds (1996).

The probabilities of the null hypothesis are equivalent ($\sim 0.46-0.5$), so neither is statistically better although the Power-law model has a slightly lower probability.

Based solely on the statistical quality of the fit, the power-law model is slightly better.

Discussion

The bremsstrahlung model suggests a thermal emitter like a **coronally active star** or **CV**. The power-law model with soft $\Gamma \approx 2.6$ is little bit higher than what we would expect for a CV but it does not rule it out. So, it could point to a **quiescent accreting system** (maybe like a **CV**) or **X-ray binary**.

The gauss models are well fitting at energies corresponding to iron lines. Nevertheless, we cannot conclude on their presence because the only two points on the spectrum are at 5 keV and 8 keV which is a very broad energy band for a very narrow iron line. If the presence of iron line was confirmed it would support the **CV** hypothesis.

The Apec model fits very badly which rule out **active stars**.

X-ray Flux and X-ray-to-Optical Flux Ratio

Optical flux

The source is detected by Gaia DR3 with a magnitude $G = 19.6951$, a faint object which is consistent with a low-mass star at 340 pc .

The G-band corresponds to the wavelength interval of: 330 nm to 1050 nm (<https://gaia.obspm.fr/la-mission/les-resultats/article/les-observations-spectro-photometriques>).

The optical flux is calculated as follow:

$$F_{\text{optical}} = F_0 * 10^{-0.4 * G} \quad (3)$$

With $F_0 = 1.05 * 10^{-5}$ Gaia zero-point magnitude.

Here, we have an optical flux of $F_{\text{optical}} \approx 1.39 * 10^{-13} \text{ erg/cm}^2/\text{s}$.

Typical X-ray flux to optical flux ratio

The typical X-ray flux to optical flux ratio of different sources is summaries in the following table:

Object type	Typical L_x range (erg/s)
Active stars	< 0.1
Cataclysmic variables	$\sim 0.1 - 10$
AGNs	> 1

X-ray flux to optical flux ratio of our source

Chi-squared

From *Xspec* AllModels.calcFlux(".2 12.0") we obtain the X-ray flux:

- Powerlaw model: $F_x \approx 4.66 * 10^{-14} \text{ erg/cm}^2/\text{s}$,
- Bremsstrahlung model: $F_x \approx 4.06 * 10^{-14} \text{ erg/cm}^2/\text{s}$,

So, an X-ray flux of $F_x \approx 4 * 10^{-14} \text{ erg/cm}^2/\text{s}$ regardless of the model.

Then, we calculate the X-ray to optical flux ratio:

- Powerlaw model: $\frac{F_x}{F_{\text{optical}}} \approx 0.34$.
- Bremsstrahlung model: $\frac{F_x}{F_{\text{optical}}} \approx 0.29$.

So, an X-ray to optical flux ratio of $\frac{F_x}{F_{\text{optical}}} \approx 0.3$ regardless of the model.

Discussion

This value doesn't contradict a CV interpretation:

- It supports a faint X-ray, optically visible Galactic object,
- It weakens the AGN hypothesis, which would typically show higher X-ray to optical dominance,
- It might slightly disfavour a highly magnetic CV, but a non-magnetic or mildly magnetic CV is still very plausible.

Luminosity

Typical luminosity

The typical luminosity of different sources is summaries in the following table:

Object type	Typical L_x range (erg/s)
Active stars	$\sim 10^{28} - 10^{30}$

Cataclysmic variables	$\sim 10^{30} - 10^{33}$
Quiescent X-ray Binaries	$\sim 10^{31} - 10^{33}$
AGNs	$> 10^{42}$

Luminosity of our source

In order to calculate the luminosity L in erg/s , the source is assumed to be spherical:

$$L = 4\pi F_X d^2 \quad (4)$$

With F_X the X-ray flux calculated previously in $erg/cm^2/s$ and d the distance to the source in cm . This distance is calculated from value of the parallax given by Gaia: $P = 2.941 mas$. We get a distance of $d \approx 1.05 * 10^{21} cm$.

Chi-squared

The luminosity of the source is:

- Powerlaw model: $L_X \approx 6.44 * 10^{29} erg/s$,
- Bremsstrahlung model: $L_X \approx 5.63 * 10^{29} erg/s$.

So, a luminosity of $L_X \approx 6 * 10^{29} erg/s$ regardless of the model.

Discussion

This luminosity is at the very low end (or even below) of **CVs** typical luminosity. It is more consistent with **active stars**.

Documentations and Catalogues

Antonio C. Rodriguez paper

<https://doi.org/10.1088/1538-3873/ad357c>

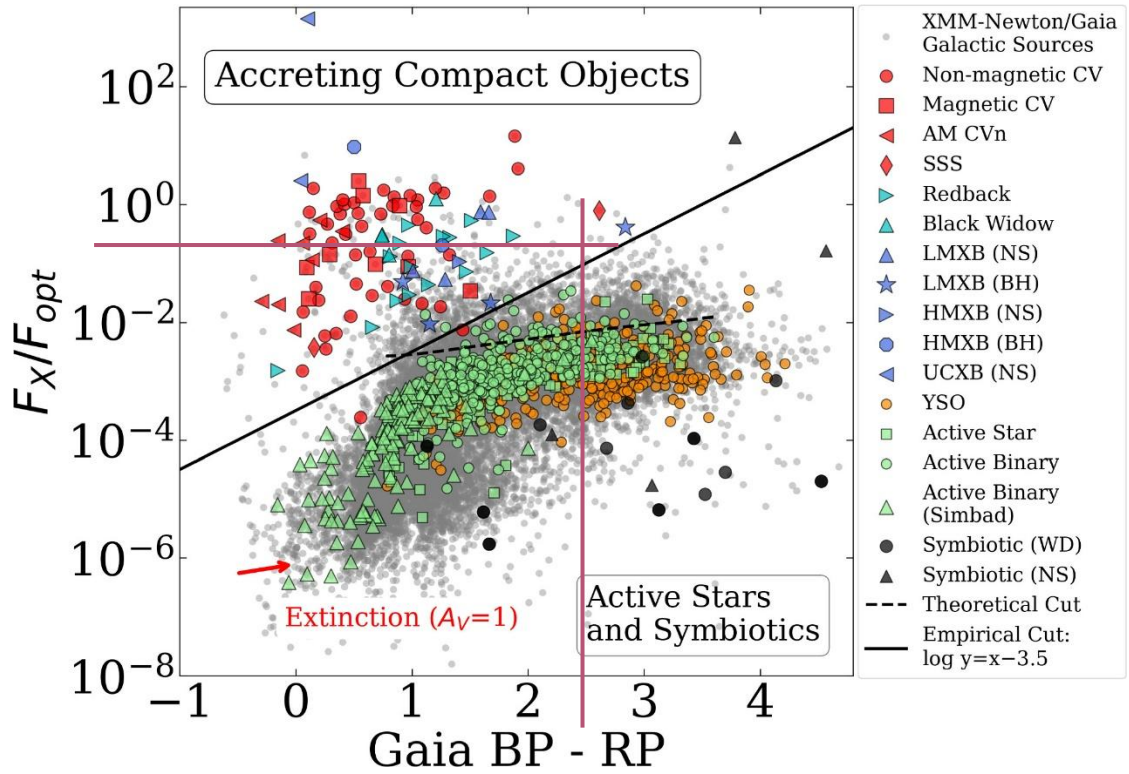


Figure 1. X-ray Main Sequence. Galactic sources from the XMM-Newton/Gaia crossmatch are shown in grey. Accreting compact object binaries in the upper left are separated from symbiotic and active stars on the bottom right by the “empirical cut” (solid line) or “theoretical cut” (dotted line). All classifications on the right-side panel are from the literature, and described in Section 2.3. No extinction correction is applied here, but the extinction vector is shown (de-reddening slides sources toward the lower left).

Gaia gives: $G_{BP} - G_{RP} = 2.416$ and we previously calculated the ratio: $\frac{F_X}{F_{optical}} \approx 0.3$. Reporting these values on the figure (pink lines) our source points just above the theoretical and empirical cuts indicating an **accreting compact object binary**.

There is a SSS just above our source. A supersoft X-ray source (SSS) is a WD that have a layer of steadily burning hydrogen on its surface. Its X-ray spectra have equivalent blackbody temperatures ranging from 15–80 eV, which means that little of its bolometric flux overlaps with the XMM-Newton energy range. Rodriguez used the catalog of SSSs from Kahabka & van den Heuvel (1997) and kept only those systems which have a detection in the XMM-Newton source catalog. 4 systems fulfill this condition (one is AG Dra, which is a symbiotic SSS and labeled as “symbiotic” in Figure 1).

There 3 SSSs on the figure:

- RX J0019.8+2156 (Gaia DR3 ID: 2800287654443977344),
- RX J0925.7-4758 (Gaia DR3 ID: 5422337322910734080),
- RR Tel (Gaia DR3 ID: 6448785024330499456).

The source we are looking for is the second one:

<https://sky.esa.int/esasky/?target=141.44150568741372%20-47.98250859920027&hips=XMM-Newton+EPIC+color&fov=0.17280004355754822&projection=SIN&cooframe=J2000&sci=true&lang=fr>

Gaia DR3

- Designation: Gaia DR3 5422337322910734080,

- Parallax: $P = 0.1325 \text{ mas}$,
- Distance: $d = 2577.0256 \text{ pc} \rightarrow d \approx 7.952 * 10^{21} \text{ cm}$,
- Magnitude: $G = 16.0072 \text{ mag}$.

EPIC Stacked

- Stack Catalogue Name: 4XMMs J092545.9-475817,
- IAU Name: 4XMM J092546.0-475817,
- RA: 09h 25m 45.995s,
- DEC: -47° 58' 17.54",
- Flux (0.2-12 keV): $F_X = 9.2524 * 10^{-12} \text{ erg cm}^{-2} \text{ s}^{-1}$,
- Hardness Ratio:
 - Between counts in the 0.5 – 1.0 keV and the 0.2 – 0.5 keV bands: $Hr_1 = -0.8413$,
 - Between counts in the 0.5 – 1.0 keV and the 1.0 – 2.0 keV bands: $Hr_2 = -0.8305$,
 - Between counts in the 2.0 – 4.5 keV and the 1.0 – 2.0 keV bands: $Hr_3 = -0.9671$,
 - Between counts in the 4.5 – 12.0 keV and the 2.0 – 4.5 keV bands: $Hr_4 = -0.9469$.

We can calculate the luminosity: $L_X = 4\pi F_X d^2 \approx 7.352 * 10^{33} \text{ erg s}^{-1}$.

Concerning our source:

<https://sky.esa.int/esasky/?target=53.5926619585791%20-28.920324865769405&hips=XMM-Newton+EPIC+color&fov=0.11215524915989739&projection=SIN&cooframe=J2000&sci=true&lang=fr>

There isn't an EPIC Stack pointer on ESASky so we need to calculate the hardness ratio ourself by extracting the eventlist.

<https://heasarc.gsfc.nasa.gov/w3browse/xmm-newton/xmmssc.html>

From PN data:

- Hardness Ratio:
 - $Hr_1 = -0.71875$,
 - $Hr_2 = 0.1$,
 - $Hr_3 = 0.2$,
 - $Hr_4 = 0.12$.

From MOS2 data:

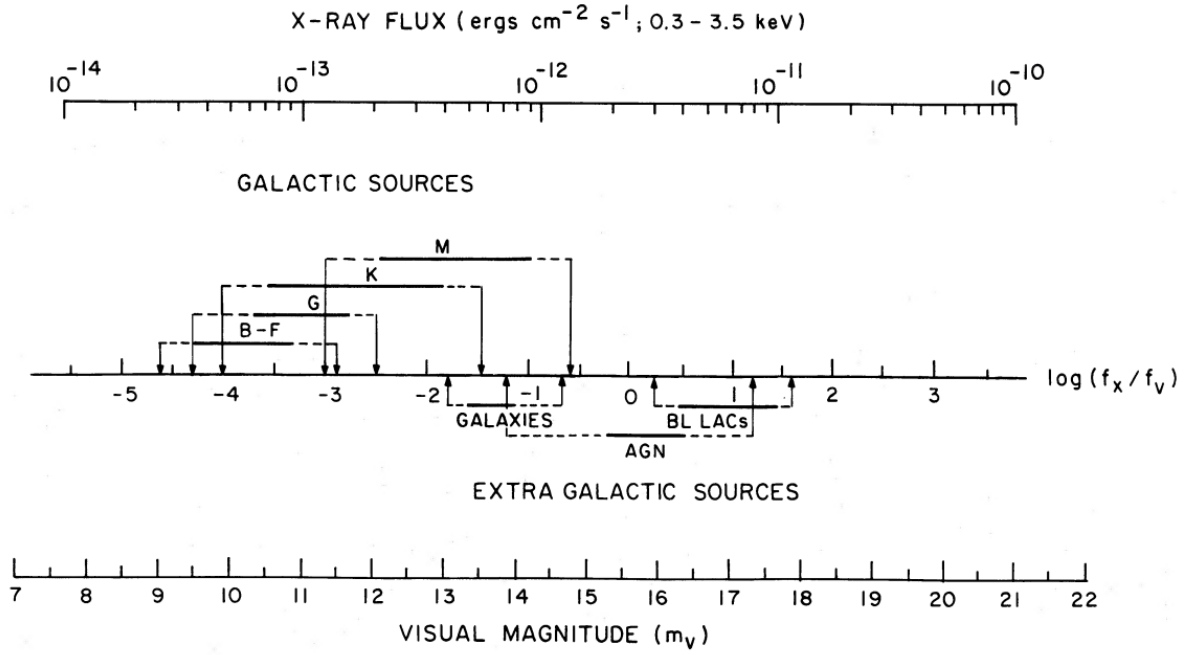
- Hardness Ratio:
 - $Hr_1 = -0.75$,
 - $Hr_2 = -1.0$,
 - $Hr_3 = 1.0$,
 - $Hr_4 = -0.14$.

PN data are more reliable in general.

We recall the luminosity found earlier: $L_X \approx 6 * 10^{29} \text{ erg/s}$.

Discussion

The values between our source and the SSS source are not matching, we can't really conclude.



$$\log (f_x / f_v) = \log f_x + \frac{m_v}{2.5} + 5.37$$

Figure 2. Nomograph to compute the $\log[f_x/f_v]$, given the X-ray flux and the visual magnitude of a source. The correspondence between the various classes of X-ray sources and their typical $\log[f_x/f_v]$ is also indicated.

The figure presents a nomograph to compute the $\log \left(\frac{f_x}{f_v} \right)$ given the X-ray flux f_x in the 0.3 – 3.5 keV band in ergs/cm²/s and the visual magnitude m_v of the source:

$$\log \left(\frac{f_x}{f_v} \right) = \log(f_x) + \frac{m_v}{2.5} + 5.37 \quad (5)$$

With f_v the visual flux.

For m_v we take the magnitude $G = 19.6951$ given by Gaia DR3, as previously.

Chi-squared

From `Xspec AllModels.calcFlux("0.3 3.5")` we obtain the X-ray flux:

- Powerlaw model: $f_x \approx 3.54 * 10^{-14} \text{ erg/cm}^2/\text{s}$.
- Bremsstrahlung model: $f_x \approx 3.59 * 10^{-14} \text{ erg/cm}^2/\text{s}$.

The logarithm is then:

- Powerlaw model: $\log (f_x/f_v) \approx -0.202$.
- Bremsstrahlung model: $\log (f_x/f_v) \approx -0.196$.

So, a logarithm of $\log (f_x/f_v) \approx -0.2$.

The Maccacaro result is ambiguous because it classifies AGN based on high X-ray-to-optical ratio; but does not exclude CVs, which have overlapping values. The majority of CVs have indeed values between $\log(f_X/f_V) \approx [-1; 1]$ (source?). Additionally, AGNs are extragalactic and far more luminous than the low luminosity we found, contradicting the AGN interpretation.

Dacheng Lin, Natalie Webb et al. paper

<https://dx.doi.org/10.1088/0004-637X/756/1/27>

The Dacheng Lin, Natalie Webb et al. paper discusses multi-wavelength data using X-ray hardness ratio.

XMM-Athena Catalogue

<https://xmm-ssc.irap.omp.eu/xmm2athena/catalogues/>

Unclassified.

Possible Classifications

Cataclysmic variables

CVs are binary systems where a white dwarf accretes matter from a companion star. In magnetic CVs (polars, intermediate polars), the accretion flow can produce strong shock-heated plasma, leading to hard X-ray emission.

CV is a strong candidate due to:

Source Identification, Counterparts and Properties

- Galactic counterpart with stellar classification,
- Multiwavelength detection: EPIC Stack (Soft X-ray), XMM-SUSS 6.2 (UV to Optical), Gaia DR3 (Optical), Euclid MER Q1 (Optical to Near-IR), 2MASS (Near-IR) and AllWISE (Near-IR to Mid-IR),
- Distance from parallax $P = 2.941 \text{ mas} \rightarrow d \approx 340 \text{ pc}$, so it is most likely Galactic,
- Gaia DR3 classification as a star.

X-ray Variability and Periodicity

- Period of 5000 s.

X-ray Spectral Properties

- Spectral fits consistent with thermal emission (Bremsstrahlung) and soft power-law
- Spectral fits consistent with Gauss + Bremsstrahlung model indicating a possible iron line emission,
- Moderate absorption: $n_H \approx 10^{20} - 10^{21} \text{ cm}^{-2}$,
- X-ray flux: $F_X \approx 4 * 10^{-14} \text{ erg/cm}^2/\text{s}$,
- X-ray to optical flux ratio: $\frac{F_X}{F_{\text{optical}}} \approx 0.3$, supporting non-magnetic or mildly magnetic CV,
- Accreting compact object binary area (above the empirical cuts) of Antonio C. Rodriguez paper figure 1,
- Value $\log(f_X/f_V) \approx -0.2$ within the $[-1; 1]$ range of CVs (Maccaro paper).

However, the soft power law index of $\Gamma \approx 2.5 - 2.6$ and the thermal emission of $k_T \approx 1.4 - 1.6 \text{ keV}$ are a bit higher than what we would expect for CVs, but do not rule them out. The luminosity $L_X \approx 10^{29} \text{ erg/s}$ is at the very low end (even below) of CVs' luminosity range, even in quiescence.

Active Star

Active star is a strong candidate due to:

Source Identification, Counterparts and Properties

- Galactic counterpart with stellar classification,
- Multiwavelength detection: EPIC Stack (Soft X-ray), XMM-SUSS 6.2 (UV to Optical), Gaia DR3 (Optical), Euclid MER Q1 (Optical to Near-IR), 2MASS (Near-IR) and AllWISE (Near-IR to Mid-IR),
- Faint: $G = 19.6951$,
- Distance from parallax $P = 2.941 \text{ mas} \rightarrow d \approx 340 \text{ pc}$, so it is most likely Galactic,
- Gaia DR3 classification as a star.

X-ray Variability and Periodicity

- Period of 5000 s, could match stellar rotation or binary orbit.

X-ray Spectral Properties

- Spectral fits consistent with thermal emission (Bremsstrahlung) and soft power law,
- Soft power law index: $\Gamma \approx 2.5 - 2.6$ and thermal emission: $k_T \approx 1.4 - 1.6 \text{ keV}$, fit with coronal emission of active stars,
- Moderate absorption: $n_H \approx 10^{20} - 10^{21} \text{ cm}^{-2}$,
- X-ray flux: $F_X \approx 4 * 10^{-14} \text{ erg/cm}^2/\text{s}$,
- Luminosity $L_X \approx 10^{29} \text{ erg/s}$ matches active stars.

However, the X-ray to optical flux ratio: $\frac{F_X}{F_{\text{optical}}} \approx 0.3$ is high for active stars. Moreover, Rodriguez paper figure 1 shows that the source is more an accreting compact object binary and the value of $\log(f_X/f_V) \approx -0.2$ is too high for M-star (Maccaro paper). Finally, the fact that Apec model does not fit disfavors even more the active star hypothesis.

References

Astronomical databases

XMM-Newton Science Archive (<https://nxs.a.esac.esa.int/nxs-a-web/#search>).

ESASky (<https://sky.esa.int/esasky/?target=53.59466666666666%20-28.902777777777782&hips=DSS2+color&fov=1&projection=SIN&cooframe=J2000&sci=true&lang=fr>).

3DNHTOOL (<http://astro.uni-tuebingen.de/nh3d/nhtool>).

XMM-Athena catalogue (<https://xmm-ssc.irap.omp.eu/xmm2athena/catalogues/>).

Journal

ScienceDirect (<https://www.sciencedirect.com/topics/earth-and-planetary-sciences/plasma-temperature>).

Scientific papers

Kado-Fong, E. et al. (2016), *M Dwarf Activity in the Pan-STARRS1 Medium-Deep Survey: First Catalog and Rotation Periods*, The Astrophysical Journal, Volume 833, Issue 2, article id. 281, 19 pp. (<https://ui.adsabs.harvard.edu/abs/2016ApJ...833..281K/abstract>).

Antonio C. Rodriguez (2024), *From Active Stars to Black Holes: A Discovery Tool for Galactic X-Ray Sources*, PASP **136** 054201 (<https://doi.org/10.1088/1538-3873/ad357c>).

Tommaso Maccacaro et al. (1988), *The X-ray spectra of the extragalactic sources in the einstein extended medium sensitivity survey*, The Astrophysical Journal, 326:680-690 (<https://articles.adsabs.harvard.edu/pdf/1988ApJ...326..680M>).

Dacheng Lin et al. (2012), *Classification of x-ray sources in the XMM-Newton serendipitous source catalog*, ApJ **756** 27 (<https://dx.doi.org/10.1088/0004-637X/756/1/27>

L. Mignon et al. (2023), *Characterisation of stellar activity of M dwarfs. I. Long-timescale variability in a large sample and detection of new cycles*, A&A 675, A168 (<https://doi.org/10.1051/0004-6361/202244249>).

Emily K. Pass et al. (2023), *Active Stars in the Spectroscopic Survey of Mid-to-late M Dwarfs within 15 pc*, The Astronomical Journal, 166:16 (14pp) (<https://iopscience.iop.org/article/10.3847/1538-3881/acd6a2>).

Website

<https://gaia.obspm.fr/la-mission/les-resultats/article/les-observations-spectro-photometriques>